Soil Dynamics and Earthquake Engineering 92 (2017) 165–175

Contents lists available at ScienceDirect

Soil Dynamics and Earthquake Engineering

journal homepage: www.elsevier.com/locate/soildyn

# A model for estimating horizontal aftershock ground motions for active crustal regions

Byungmin Kim[a], Moochul Shin[b,*]

[a] Department of Civil, Environmental, and Construction Engineering, Texas Tech University, Box 41023, Lubbock, TX 79409, USA
[b] Department of Civil and Environmental Engineering, Western New England University, 1215 Wilbraham Rd, Springfield, MA 01119 USA

ARTICLE INFO

*Keywords:*
Aftershock
Active crustal region
Ground motion prediction
NGA-West2
Spectral acceleration

ABSTRACT

Inconsistent observations on the characteristics of ground motions from aftershocks have been found, while there is increasing attention to effects of aftershock ground motions on structural behaviors. This study examines differences in ground motions from main shock and aftershock earthquakes using the NGA-West2 database, and propose an empirical model to estimate the average horizontal components of peak ground acceleration (*PGA*), and peak ground velocity (*PGV*), and 5% damped pseudo spectral acceleration (*PSA*) at various spectral periods of aftershock earthquakes for tectonically active crustal regions, as a function of aftershock to main shock magnitude ratio, distance ratio, and time-averaged shear-wave velocity in the upper 30 m of soil deposits ($V_{S30}$). Spectral accelerations from aftershock earthquakes are smaller than those from main shock earthquakes given the same magnitude, especially at short periods. Performance of the proposed model is evaluated using a mixed-effects residuals analysis. Period-dependent standard deviation of residuals is also presented.

## 1. Introduction

Large earthquakes are often followed by aftershocks [e.g., [1–5]]. A series of aftershock earthquakes can cause severe damage on structures that were already weakened by main shock events. Historical seismic events demonstrated the vulnerability of existing structures including buildings and bridges when they were subjected to a main shock followed by series of aftershocks [e.g., [6–9]]. For example, aftershocks during the 2011 Christchurch earthquake in New Zealand aggravated damage on Christchurch and the central city area economically and structurally [e.g., [9,10]]. Therefore, many researchers have studied responses of structures (e.g., reinforced concrete (RC) buildings, concrete gravity dams) subject to sequential earthquake loadings [e.g., [11–16]]. Among these studies, Ruiz-García [1] used actual ground motion records from main shock and aftershock earthquake sequences in Mexico, including the **M**8.0 1985 Michoacán earthquake, and showed that the changes of predominant periods in aftershock ground motions affect structural responses. Hatzigeorgiou and Liolios [2] also examined the behavior of RC framed structures using ground motion records from five real seismic sequences in the U.S. However, aftershock ground motion records are not always available, and often have to be computed and/or synthesized, especially for forward prediction analyses. Therefore, it is import to adequately estimate ground motion intensity measures (e.g., peak ground acceleration (*PGA*), peak ground velocity (*PGV*), and spectral acceleration) of aftershock earthquakes. Appropriately characterizing aftershock ground motions allows precise evaluation of seismic performances of structures subjected to main shock-aftershock sequential loadings. However, there have been only a few limited approaches to estimate aftershock ground motions for main shock-aftershock sequential analyses.

One of the common approaches to obtaining aftershock ground motion time series is to repeat main shock ground motion time series using frequency-invariant scaling factors [e.g., [3,4]]. Another common approach is to randomly select time series from a set of main shock records and scaling them down to achieve desired amplitudes for aftershock motions. [e.g., [2,4,5]]. However, these conventional approaches are not capable of obtaining ground motion time series properly representing characteristics of aftershock ground motions because the frequency contents of aftershock ground motions usually differ from those of main shock ground motions. Hatzigeorgiou and Besko [6] used a ground motion prediction equation to find the PGA scaling factors for different earthquake magnitudes. However, the ground motion prediction equation is developed only for main shock earthquakes.

It is well recognized that earthquakes with smaller magnitudes

* Corresponding author.
*E-mail address:* moochul.shin@wne.edu (M. Shin).

http://dx.doi.org/10.1016/j.soildyn.2016.09.040
Received 7 August 2015; Received in revised form 29 July 2016; Accepted 25 September 2016

produce ground motions with shorter predominant periods (due to reduction in long period components) than those with larger magnitudes. Therefore, it is not surprising to observe that ground motions from aftershock earthquakes, whose magnitudes are smaller than those of main shocks, have shorter predominant periods than main shock ground motions. Goda and Taylor [7] showed that spectral accelerations of aftershocks at long periods are smaller than those of main shocks. However, there are inconsistent observations on the differences between aftershock and main shock ground motions if the magnitudes are similar. Atkinson [8] observed from regional seismograph records in Eastern North America that high-frequency spectral accelerations from aftershock earthquakes are smaller than those from main shocks given the same magnitude. On the other hand, Douglas and Halldorsson [9] have found that the differences in ground motions from main shocks and aftershocks are insignificant using the strong motion data from Europe, the Mediterranean area, and the Middle East.

Similar controversial observations are found in the recently developed Next Generation Attenuation relationships for the Western United States (NGA-West2) ground motion prediction equations (GMPEs): (1) Boore et al. [10], Campbell and Bozorgnia [11], Chiou and Youngs [12] removed aftershocks when developing GMPEs; (2) Idriss [13] included aftershock motions, but did not differentiate those from main shock motions; (3) Abrahamson et al. [14] included aftershock motions and provided scaling factors for aftershock motions. Abrahamson et al. [14] proposed period-dependent scaling factors that reduces main shock ground motions at short periods (T < ~0.6 s) and increases those at relatively longer periods (T > ~0.6 s).

Given the lack of appropriate approaches for obtaining aftershock ground motions and inconsistent observations on the characteristics of ground motions between main shocks and aftershocks, this study systematically examines the differences in ground motions from main shock and aftershock earthquakes (more than 5500 records) using the NGA-West2 database [15], and proposes a predictive model for estimating aftershock motion intensity measures given the information of main shock earthquakes. This will enhance a methodology for selecting/generating aftershock ground motion time series for dynamic analyses of structures subjected to main shock-aftershock sequential loadings.

## 2. Data set selection

Ground motion data in active crustal regions (ACRs) were selected from the Next Generation Attenuation relationships for the Western United States (NGA-West2) database [15]. Aftershock events were defined as those having a Centroid Joyner-Boore distance ($CR_{JB}$) less than 20 km [16]. Abrahamson et al. [17] used a $CR_{JB} < 15$ km as an aftershock selection criterion. It was found that the criteria of using 10 km and 20 km did not yield differences in the ratios of pseudo spectral accelerations (PSAs) as shown in Appendix A (see Figs. A.1 and A.2).

By adopting the criterion of $CR_{JB} < 20$ km, earthquakes with great magnitude can be considered as aftershocks. Although it is known that an aftershock with the magnitude greater than 7.0 is rare, the 1999 **M**7.1 Düzce earthquake, Turkey that occurred on 12 November 1999 was especially included as an aftershock event in this study. Some researchers consider the 1999 Düzce earthquake is a totally independent earthquake separated from the 1999 Kocaeli earthquake (also known as the 1999 Izmit earthquake) with the magnitude of 7.4, since the broken branches of the North-Anatolian fault (NAF) were different [18]. However, some researchers found that the 1999 Düzce earthquake had similar characteristics to those of the aftershocks of the 1999 Kocaeli earthquake despite the differently broken NAF branches. The researchers concluded that the 1999 Düzce event was highly affected by the 1999 Kocaeli earthquake [e.g., [19,20]]. Therefore, herein, the 1999 Düzce earthquake is categorized as an aftershock event. The analyses shows no significant differences for the 1999 Düzce earthquake compared to other aftershock earthquakes (see Figs. A.1 and A.2).

The data only with good quality flags were used herein, as specified in the flat file of the NGA-West2 project [21]. The data considered to be not applicable to active crustal regions identified by Abrahamson et al. [17] were excluded from the database. The data recorded at stations that are not representative of free-field conditions were also excluded as described by Boore et al. [22]. The final data set used in this study consists of 2817 pairs of main shock and aftershock ground motions (recorded at the same stations) from 140 aftershocks and 39 main shocks. Among these records, 490 pairs are from the state of California, U.S.A, 100 pairs from the Mediterranean region (Italy and Turkey), 923 pairs from China, 1303 pairs from Taiwan, and one from Nicaragua. Fig. 1 shows the epicenters of the main shock and aftershock earthquakes..

Fig. 2(a) shows a distribution of moment magnitude (**M**) and rupture distance ($R_{rup}$) of selected records of the main shocks and aftershocks. Magnitudes of the main shock earthquakes range from 3.2 to 7.9, while those of the aftershock earthquakes range from 3.0 to 7.1. The range of the rupture distances of the main shock records is from 1.6 to 473 km, while those of the aftershock records from 3.8 to 496 km. Time-averaged shear-wave velocities for the top 30 m soil deposits ($V_{S30}$) of recording stations from the NGA-West2 database which are based on both measurements and estimates by various proxy methods were considered [23]. Values of $V_{S30}$ at the selected recording stations vary from 124 m/s to 1526 m/s with the concentration in the range of 200–700 m/s as shown in Fig. 2(b)..

Peak ground acceleration (PGA), peak ground velocity (PGV), and 5% damped pseudo spectral accelerations (PSAs) at 23 oscillator periods ($T$) from 0.01 to 10 s were used. These ground motion intensity measures are averages of two horizontal ground motion records referred to as RotD50, the 50th percentile of the two measures over all non-redundant rotation angles [21].

## 3. Ratio of *PSAs* of aftershocks to main shocks

The response spectra of the 1994 Northridge, California earthquake and its four aftershock earthquakes recorded at station Castaic-Old Ridge Route are shown in Fig. 3(a) as an example. The pseudo-spectral accelerations (*PSA*s) of the four aftershock earthquakes are less than that of the main shock earthquake because of the reduced earthquake magnitudes and longer rupture distances. The ratios of $PSA^{AS}$ to $PSA^{MS}$ (the superscripts, AS and MS, denote aftershock and main shock, respectively) at long periods are smaller than those at the short periods as shown in Fig. 3(b). The ratios of $PSA^{AS}$ to $PSA^{MS}$ normalized based on the average of NGA-W2 models that do not account for aftershocks (i.e., Boore et al. [10], Campbell and Bozorgnia [11], and Chiou and Youngs [12]) are shown in Fig. 3(c). With the normalization, the $PSA^{AS}$ values are still smaller than the $PSA^{MS}$ values, especially at long periods. Fig. 4 shows $PSA^{AS}/PSA^{MS}$ for all 2817 paired records, and it clearly demonstrates the period dependency of $PSA^{AS}/PSA^{MS}$. The $PSA^{AS}/PSA^{MS}$ slightly increases with respect to period when the

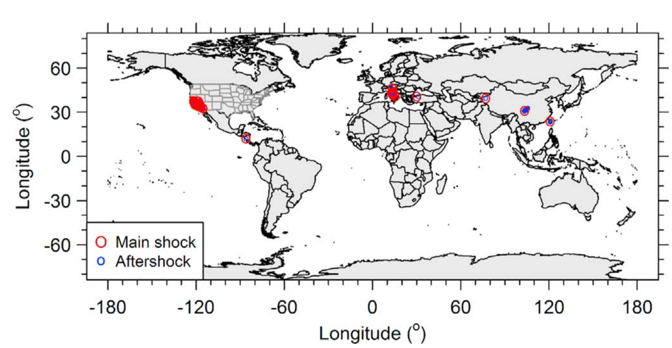


**Fig. 1.** Epicenters of the main shocks and aftershocks used in this study.